


ECM-enriched alginate hydrogels for bioartificial pancreas: an ideal niche to improve insulin secretion and diabetic glucose profile

Journal of Applied Biomaterials &
Functional Materials
October-December: 1–13
© The Author(s) 2019
Article reuse guidelines:
sagepub.com/journals-permissions
DOI: 10.1177/2280800019848923
journals.sagepub.com/home/jbf


Joana Crisóstomo¹, Ana M Pereira¹, Sílvia J Bidarra^{2,3},
Ana C Gonçalves^{4,5,6}, Pedro L Granja^{2,3,7,8}, Jorge FJ Coelho⁹,
Cristina C Barrias^{2,3,8} and Raquel Seça¹

Abstract

Introduction: The success of a bioartificial pancreas crucially depends on ameliorating encapsulated beta cells survival and function. By mimicking the cellular *in vivo* niche, the aim of this study was to develop a novel model for beta cells encapsulation capable of establishing an appropriate microenvironment that supports interactions between cells and extracellular matrix (ECM) components.

Methods: ECM components (Arg-Gly-Asp, abbreviated as RGD) were chemically incorporated in alginate hydrogels (alginate-RGD). After encapsulation, INS-IE beta cells outcome was analyzed *in vitro* and after their implantation in an animal model of diabetes.

Results: Our alginate-RGD model demonstrated to be a good *in vitro* niche for supporting beta cells viability, proliferation, and activity, namely by improving the key feature of insulin secretion. RGD peptides promoted cell–matrix interactions, enhanced endogenous ECM components expression, and favored the assembly of individual cells into multicellular spheroids, an essential configuration for proper beta cell functioning. *In vivo*, our pivotal model for diabetes treatment exhibited an improved glycemic profile of type 2 diabetic rats, where insulin secreted from encapsulated cells was more efficiently used.

Conclusions: We were able to successfully introduce a novel valuable function in an old ally in biomedical applications, the alginate. The proposed alginate-RGD model stands out as a promising approach to improve beta cells survival and function, increasing the success of this therapeutic strategy, which might greatly improve the quality of life of an increasing number of diabetic patients worldwide.

Keywords

Diabetes, bioartificial pancreas, alginate hydrogels, extracellular matrix, beta cells

Date received: 10 May 2018; revised: 15 April 2019; accepted: 17 April 2019

¹IBILI - Institute for Biomedical Imaging and Life Sciences, University of Coimbra, Coimbra, Portugal

²i3S - Instituto de Investigação e Inovação em Saúde, Universidade do Porto, Porto, Portugal

³INEB - Instituto de Engenharia Biomédica, Porto, Portugal

⁴University Clinic of Hematology and Applied Molecular Biology Unit, University of Coimbra, Coimbra, Portugal

⁵CIMAGO - Centre of Investigation in Environment Genetics and Oncobiology, University of Coimbra, Coimbra, Portugal

⁶CNC.IBILI - Center for Neuroscience and Cell Biology, University of Coimbra, Coimbra, Portugal

⁷FEUP - Faculdade de Engenharia, Universidade do Porto, Porto, Portugal

⁸ICBAS - Instituto de Ciências Biomédicas Abel Salazar, Universidade do Porto, Porto, Portugal

⁹CEMUC - Centre for Mechanical Engineering of the University of Coimbra, University of Coimbra, Coimbra, Portugal

Corresponding author:

Joana Crisóstomo, Laboratory of Physiology, IBILI - Institute for Biomedical Imaging and Life Sciences, Faculty of Medicine, University of Coimbra, Pólo III - Azinhaga Santa Comba, Celas, 3000-548 Coimbra, Portugal.
Email: joanacrisostomo@hotmail.com



Introduction

Transplantation of insulin-producing cells has shown potential to become a widely applicable treatment for diabetes.¹ Nevertheless, this procedure is still associated with a high rate of graft failure, mainly caused by immune attack and poorly functioning cells.² With a bioartificial pancreas the immune attack is attenuated; however, graft failure is still frequently reported.¹ During the isolation procedure, the islets' microenvironment is destroyed and the loss of extracellular matrix (ECM) impairs cells functioning and survival.³ The lack of ECM components is even more problematic when individualized beta cells are used off the islets supportive microenvironment. The advantage of using beta cells (from cell lines or derived from stem/pluripotent cells) is that it could be an inexhaustible and immunocompatible source of beta cells, solving the lack of islets donors and the rejection issue, in the case of autologous source. Therefore, for bioartificial pancreas success, using islets or individualized beta cells is crucial to re-establish and favor the interaction between cells and ECM, by closely mimicking the complex *in vivo* three-dimensional (3D) microenvironment.^{4,5}

The ECM is associated with cell survival, morphology, growth, migration, function, and differentiation processes.⁶ Likewise, cell-ECM interactions are mandatory for survival and proper functioning of insulin-secretion cells. Collagen I, collagen IV, laminin, and fibronectin lead to increments in viability and insulin production, both in individual beta cells and islets from human and animal models.⁷⁻¹⁰ Nevertheless, islets beta cells are unable to form an ECM basement membrane, which is damaged during the isolation and absent in disaggregated beta cells.⁷ Moreover, the treatment with laminin improves MIN6 beta cells functioning in an integrin dependent manner, highlighting the crucial importance of ECM components to cellular maintenance.⁷ The increment of insulin-producing cells functioning, favored by their interaction with ECM, has already been reported in two-dimensional (2D) and 3D models of cellular encapsulation.¹⁰⁻¹³ 3D spherical models of alginate hydrogels are the most frequently and successfully used in beta cells encapsulation and have already been applied in clinical studies.¹⁴⁻¹⁶ Accordingly, modification of alginate hydrogels by incorporating ECM components is a promising approach to improve cell survival and function, and increase the success of this therapeutic strategy.¹⁷⁻²¹

Tripeptide Arg-Gly-Asp (RGD) is present in ECM proteins like fibronectin, laminins, collagen type I, vitronectin, and fibrinogen, and approximately one-third of integrin receptor family recognizes this adhesion peptide.²² Addition of soluble RGD peptide to culture medium was shown to improve the resistance of rat islets against apoptosis.¹⁰ Culturing beta cells in 2D models also demonstrated to improve insulin secretion in different beta cell lines: in INS-1E cultured in surfaces coated with RGD,²³

in MIN6 cultured in surfaces coated with self-assembled peptide amphiphiles inscribed with RGD,²⁴ and in β -TC6 cultured in surfaces coated with RGD-modified elastin-like polypeptide.²⁵ In 3D models of poly(ethylene glycol) (PEG) hydrogels, the presence of RGD also ameliorated MIN6 beta cells viability.²⁶ Despite the promising results of these approaches and the long-time reported attractiveness of alginate hydrogels for beta cells encapsulation, the introduction of these adhesive peptides in alginate for bioartificial pancreas development has only recently been reported.²⁷ Llacua et al. showed supported human islets function with physical entrapment of ECM components in alginate microcapsules, namely RGD peptides.²⁷ In the present work we introduced a more stable and efficient method to incorporate RGD peptides which were chemically linked to alginate backbone. Moreover, besides the *in vitro* validation, we were able to assess the *in vivo* performance of our approach.

Therefore, the aim of this study was to investigate the potential of a new model of alginate hydrogels chemically grafted with RGD (alginate-RGD) as an optimal 3D niche for INS-1E beta cells encapsulation and allow transplantation to type 2 diabetic rats (Goto-Kakizaki, GK). Rat INS-1 cells, which were already tested in encapsulation studies *in vitro*,^{28,29} can be differentiated in stable INS-1E cells. Due to their high insulin content and secretory responses in the physiological glucose concentration range,³⁰ INS-1E cells constitute a good model for both *in vitro* and *in vivo* studies. The GK model is characterized by morphofunctional alterations in beta cells leading to a deficit in insulin secretion pattern, being also a good model to test bioartificial pancreas usefulness. *In vitro*, the positive effect of RGD peptides on beta cells performance was proved, boosting the *in vivo* validation.

Materials and methods

Synthesis of alginate-RGD

Sodium alginate (PRONOVA Ultrapure Sodium Alginate LVG, Batch no: FP-606-02, Product no: 4200001, NovaMatrix, FMC Biopolymers) with high guluronate content ($\approx 68\%$) was used in alginate-RGD synthesis. Cell-adhesion peptide (glycine)₄-arginine-glycine-aspartic acid-serine-proline (abbreviated as RGD, GenSript) was grafted to alginate using carbodiimide chemistry, as described in detail in previous studies.³¹⁻³³ Briefly, a 1% (m/v) alginate solution in MES buffer (0.1 M MES, 0.3 M NaCl, pH = 6.5) was prepared and stirred overnight at room temperature. Per g of alginate, 27.4 mg of Sulfo-NHS, 48.42 mg of EDC, and 16.7 mg of RGD peptide were sequentially added. After stirring for 20 h, the reaction was quenched with NH₂OH. During the subsequent 3 days, unreacted species were separated by dialysis (MWCO 3500) against solutions of decreasing concentration of NaCl and finally deionized water. At the end, RGD-alginate was lyophilized and stored at -20°C until further use. The

reaction yield was calculated using the BCA Protein Assay (Pierce), as previously described.³³ Briefly, samples were incubated with BCA reagent for 60 min at 37°C in the dark and the absorbance was read at 540 nm in a microplate reader (Biotek Synergy MX). For calibration curve, standard solutions were prepared with RGD peptide concentration ranging from 0 to 1 mg/mL in 1% (m/v) alginate. The efficiency of the coupling process was calculated as:

$$\text{efficiency (\%)} = (\text{grafted peptide} / \text{input peptide}) \times 100.$$

Cell culture

INS-1E beta cells from rat insulinoma were cultured at 37°C under a 5% CO₂ humidified atmosphere, in RPMI 1640 medium, supplemented with 10% (v/v) fetal bovine serum, 100 U/mL penicillin + 100 µg/mL streptomycin, 10 mM HEPES, 1 mM sodium pyruvate, and 50 µM of β-mercaptoethanol.

Cell encapsulation

Alginate for cell encapsulation was prepared in 0.9% (m/v) NaCl at a final concentration of 2% (m/v), containing 0 or 200 µM of RGD peptide (Alg-0 or Alg-RGD, respectively). Briefly, trypsinized cells corresponding to a concentration of 5×10^6 cells/mL were carefully mixed with alginate solution and the mixture was extruded under a coaxial nitrogen flow using a Var J1 encapsulation unit (Nisco),³⁴ or through a 25G needle (for *in vitro* and *in vivo* studies, respectively). Alginate hydrogels were cross-linked in an isotonic solution with 100 mM CaCl₂ and 10 mM HEPES during 15 min, washed and cultured under standard conditions. For size and shape evaluation, spheres were observed through microscopy (stereo microscope SZX10, Olympus, and inverted microscope Axiovert, Zeiss). Photographs were captured, and software Image J was used for diameter measurement.

In vitro behavior of encapsulated cells

Cell viability. Cell viability was assessed by live/dead assay (Invitrogen), performed at days 1 and 7, according to the manufacturer's instructions. Briefly, microspheres were washed and incubated at 37°C with 1 mM calcein AM to stain live cells and 2.5 mM ethidium homodimer-1 (EthD-1) to stain dead cells. After 45 min, the supernatant was replaced by fresh medium and, at the time of analysis, the medium was changed to TBST with CaCl₂ (TBS-Ca) (150 mM NaCl, 50 mM Tris, 7.5 mM CaCl₂, pH = 7.4). Whole-mounted samples were imaged by confocal laser scanning microscopy (CLSM; Leica SP2 AOBS).

Metabolic activity. Cell metabolic activity was assessed at days 1, 4, and 7 by resazurin assay. Hydrogels were incubated with

20% (v/v) of resazurin solution (0.1 mg/mL) in RPMI medium for 2 h at 37°C. Supernatant fluorescence was read in a black 96-well plate with clear bottom using a microplate reader (Biotek Synergy MX) with Ex/Em at 530/590 nm.

Cell proliferation. To evaluate cell proliferation, total double-stranded DNA (dsDNA) was quantified at days 1, 4, and 7. Hydrogels were dissolved with 0.25% (m/v) trypsin/50 mM EDTA and INS-1E cells were recovered after washes with PBS (137 mM NaCl, 2.7 mM KCl, 10 mM Na₂HPO₄, 2 mM KH₂PO₄, pH = 7.4) and centrifugations (400g, 5 min), and stored at -20°C. Cells were lysed in 1% (v/v) Triton X-100 for 1 h at 400 r/min at 4°C and dsDNA was quantified using the Quant-iT PicoGreen dsDNA kit (Invitrogen), according to manufacturer's instructions. Briefly, samples were transferred to a black 96-well plate with clear bottom and diluted in TE buffer (200 mM Tris-HCl, 20 mM EDTA, pH = 7.5). Then the Quant-iT PicoGreen dsDNA reagent was added and samples were incubated for 5 min at room temperature in the dark. Fluorescence was quantified using a microplate reader (Biotek Synergy MX) with Ex/Em at 480/520 nm. The measured fluorescence units were converted into samples dsDNA (ng/mL) using a standard curve of DNA in the range 1–1000 ng/mL.

Glucose-stimulated insulin secretion (GSIS). A GSIS test was performed at day 4 of culture. Media were discarded and hydrogels were carefully washed with a modified Krebs-Ringer buffer (KRB) (135 mM NaCl, 3.6 mM KCl, 0.5 mM NaH₂PO₄, 5 mM NaHCO₃, 10 mM HEPES, 1.5 mM CaCl₂, 0.5 mM MgCl₂, 0.1% (m/v) BSA) and replaced with the same buffer during 1 h. After washes, samples were incubated with KRB supplemented with glucose at low (2.8 mM) or high concentration (16.7 mM) during 1 h. All samples were collected and insulin levels were assessed using a commercial ELISA kit: Ultrasensitive Rat Insulin ELISA (Mercodia), according to the manufacturer's instructions. Briefly, after the samples incubation with anti-insulin antibody carrying peroxidase and with enzyme substrate, absorbance was read at 450 nm using a microplate reader (Biotek Synergy MX).

Gene expression. At day 7, total RNA was extracted from INS-1E cells recovered from alginate microspheres using Isolate II RNA Mini Kit (Bioline), as recommended by the manufacturer. RNA quantification was performed using a NanoDrop 1000 spectrophotometer. Subsequently, 0.5 µg of total RNA were used to convert in single-stranded cDNA by the Cloned AMV First-Strand cDNA Synthesis kit (Invitrogen). After cDNA synthesis reaction, a mixture containing cDNA, primers and SsoFast EvaGreen Supermix (Bio-Rad) was made to run qRT-PCR experiments using an CFX96 equipment (Bio-Rad) under the following conditions: 95°C for 30 s, followed by 40 cycles at 95°C

Table 1. Sequence of primers used for qRT-PCR.

Gene	Sequence of primers	Reference
<i>Ins1</i>	F: 5'-GTGGCATTGTGGATCAGT-3' R: 5'-GCTCATTCAAAGGCTTTATTCA-3'	NM_019129
<i>Pdx1</i>	F: 5'-TGGAAGAAAGAGGAAGATAAGAAA-3' R: 5'-GAGGTTACGGCACAATCC-3'	NM_022852
<i>Glut2</i>	F: 5'-GATTACTGGCACATCCTACTTG-3' R: 5'-CCTGACTTCCTCTTCCAAC-3'	NM_012879
<i>Sur1</i>	F: 5'-GCCACCTCCACTTATACA-3' R: 5'-AGAAGCTTGACGAACCTTGATG-3'	NM_013039
<i>Col1a1</i>	F: 5'-GTGCGATGGCGTGCTATG-3' R: 5'-ACTTCTGCGTCTGGTGATACA-3'	NM_053304
<i>Col4a1</i>	F: 5'-TCTTCCACCCTCTACACAGA-3' R: 5'-TCCACAGAAAGCCATGACTT-3'	NM_001135009
<i>Lama1</i>	F: 5'-GACGGTGGACAGTAATCTC-3' R: 5'-TTCTCAGGCACAAGTCTAAC-3'	NM_001108237
<i>Fn1</i>	F: 5'-AGCACAGAACTCAACCTT-3' R: 5'-CTCCTCCACAGCATAGATAG-3'	NM_019143
<i>Itga3</i>	F: 5'-GAACGATTGTGAACGCATGG-3' R: 5'-GCCAGGGTCGAGCTGTAGGT-3'	XM_340884
<i>Itgb1</i>	F: 5'-CAGATGAAGTGAACAGTGAAGACA-3' R: 5'-GTTGGACCTATCGCAGTTGAAG-3'	NM_017022

Ins1, insulin 1; *Pdx1*, pancreatic and duodenal homeobox 1; *Glut2*, glucose transporter 2; *Sur1*, sulfonylurea receptor 1; *Col1a1*, collagen type 1 alpha 1; *Col4a1*, collagen type IV alpha 1; *Lama1*, laminin alpha 1; *Fn1*, fibronectin 1; *Itga3*, integrin alpha 3; *Itgb1*, integrin beta 1; F, forward primer; R, reverse primer.

for 5 s and 60°C for 20 s. Melting curves were obtained by increasing the temperature from 50 to 95°C in increments of 0.5°C. The housekeeping gene hypoxanthine phosphoribosyltransferase 1 (*Hprt1*) was used as the endogenous assay control. The expression value for each target gene was normalized to the *Hprt1* gene and the relative quantification of gene amplification was calculated as follow: $2^{-\Delta C_t}$, represented in relation to the control expression (Alg-0). The sequence of the primer pairs used is indicated in Table 1.

Transplantation of encapsulated cells

Animals and surgical procedure. Type 2 diabetes GK rats from our local colonies (FMUC, Coimbra, Portugal) were maintained under controlled light, temperature, and humidity conditions and with free access to water and a standard diet (AO3, Panlab). The experimental protocol was approved by the local Institutional Animal Care and Use Committee of the Faculty of Medicine, University of Coimbra. All animal care and experimental procedures were performed in accordance with the Portuguese Law on Experimentation with Laboratory Animals, which is based on the principles of laboratory animal care, as adopted by Directive 2010/63/EU, and by users licensed by the Federation of Laboratory Animal Science Associations (FELASA). Rats between 22 and 26 weeks of age were divided into three experimental groups: GK control

(GKc) – control rats ($n = 4$); GK vehicle (GKv) – rats implanted with empty alginate-RGD spheres ($n = 3$); GK implanted with cells (GKi) – rats implanted with INS-1E cells encapsulated in RGD-alginate spheres ($n = 3$). 24 h after cell encapsulation, each rat was implanted with 100 spheres of about 2 mm, containing 5×10^6 cells (GKi). GKv rats received the same number of spheres without cells. The surgical procedure consisted in anaesthetizing the animals with ketamine/chlorpromazine and implantation of the spheres in the subcutaneous space located in the neck. This place has adequate space, good physical support and vascular supply and required a minor surgery. The implant remained in rat for 21 days. Allowing an easier handling, bigger spheres with the same cell density as microspheres (5×10^6 cells/mL) were used for *in vivo* implantation.

Body weight and glycaemia determination. Body weight was determined in fasted rats (6 h) at the beginning and at the end of the experimental period (21 days). Water and food intake were daily monitored during the whole period. Occasional glycaemia was evaluated, at the same hour, before implantation (day 0) and at days 1, 2, 3, 4, 5, 7, 11, 18, and 21 after implantation. Fasting glycaemia was measured after 6h of fasting, at day 0 and 21. Intraperitoneal glucose tolerance test (IPGTT) was carried before the implantation and 7 days afterwards. For that purpose, glucose (1.8 mg/kg) was intraperitoneally injected in rats and

glycaemia measured 15, 30, 60, 90, and 120 min after glucose loading. All glycemic levels were determined in tail vein peripheral blood using a glucometer and test strips (Elite, Bayer).

Blood biochemical analyses and insulinemia. Fasting blood (6 h) was collected at the end of the 21 days by cardiac puncture from anaesthetized animals. Serum and plasma were separated by centrifugation (3500g, 10 min, 4°C) in adequate tubes (BD Vacutainer and BD Vacutainer K3E EDTA, respectively) and stored at -80°C. Blood levels of urea nitrogen, creatinine, urates, total proteins, albumin, alanine transaminase, aspartate transaminase, alkaline phosphatase, and total bilirubin were measured by an automatic analyzer (Olympos Diagnóstica, Produtos de Diagnóstico SA). Insulin levels were determined by ELISA method, using a commercial kit (Ultrasensitive Rat Insulin ELISA, Mercodia), according to manufacturer's instruction. Briefly, after the samples incubation with anti-insulin antibody carrying peroxidase and with enzyme substrate, absorbance was read at 450 nm using a microplate reader (Biotek Synergy MX). The insulin-resistance (HOMA) and insulin-sensibility (QUICKI) indexes were calculated as follows:

$$HOMA = (\text{fasting insulin } (\mu\text{U} / \text{mL}) \\ \times \text{fasting glucose } (\text{mmol} / \text{L}) / 22.5$$

$$QUICKI = 1 / [\log (\text{fasting insulin } (\mu\text{U} / \text{mL}) + \\ \log (\text{fasting glucose } (\text{mg} / \text{dL}))]$$

Histological assessment. Implant and adjacent tissues were recovered at day 21, fixed in 4% (m/v) PFA (in TBS-Ca) overnight at 4°C and, after tissue processing, embedded in paraffin. Three micrometer cross-sections were obtained from all animal's explant. Hematoxylin-eosin (HE) and Masson's trichrome (MT) stainings were used to assess tissue basic structure. For insulin immunolabeling, a specific insulin antibody and detection kit MultiView mouse-HRP IHC (Enzo) were used. Briefly, after antigen recovery during 30 min at 90°C with 10 mM citrate and 0.5% (v/v) Tween 20, sections were blocked with PBS supplemented with 1% (m/v) BSA and 10% (v/v) goat sera, and incubated overnight with insulin primary antibody (mouse anti-human insulin monoclonal antibody, 1:100, BioTrend). After washings, sections were incubated with mouse-HRP during 2 h followed by incubation with DAB (3,3-diaminobenzidine) during 5 min. Then, sections were stained with HE during 8 min, washed, and prepared for microscopic analysis with aqueous medium.

Statistical analysis

Statistical analyses were performed using GraphPad software. Shapiro-Wilk and D'Agostino tests were used to assess the normal distribution of variables.

Differences were assessed by Mann-Whitney test for comparisons between two groups and by Kruskal-Wallis (Dunn's post hoc test for multiple comparisons) for comparisons between three groups. Two-way analysis of variance was used when more than one factor was considered. Wilcoxon signed-rank test was used to assess the differences in gene expression. Differences were considered statistically significant for p values <0.05. All data are presented as mean \pm standard error of mean (SEM).

Results

Effect of RGD-grafted alginate on in vitro metabolic activity, proliferation, and viability of encapsulated INS-1E cells

Produced microspheres showed a uniform spherical shape with average diameter of $1270 \pm 69 \mu\text{m}$ (Figure 1(a)). INS-1E beta cells were uniformly distributed inside hydrogels and the presence of adhesion peptide RGD showed a positive effect on cellular behavior. Comparing both encapsulation conditions (Alg-0 and Alg-RGD), levels of dsDNA, which allow assessment of cell proliferation, were significantly higher at days 4 and 7 on cells encapsulated in Alg-RGD ($p < 0.01$ and $p < 0.001$, respectively). Moreover, the significant increment of dsDNA reached the plateau earlier in RGD-free counterpart (day 4) than in Alg-RGD condition (Figure 1(b)). Accordingly, cellular metabolic activity showed a significant increase in Alg-RGD at days 4 ($p < 0.01$) and 7 ($p < 0.001$). Again, cells in contact with RGD significantly increased linearly their metabolic activity throughout the 7 days of culture, while in Alg-0 condition, a tendency to stabilize after day 4 was observed (Figure 1(c)). Cellular metabolic activity displayed a similar profile as dsDNA levels, suggesting that when increased metabolic activity was observed it might have resulted from the increased number of cells. The confocal images of Live/Dead assay confirmed the previous results. In Alg-RGD stainings there were more viable cells than in Alg-0 condition (Figure 1(d)), showing again the essential presence of such adhesive peptides. Moreover, comparing confocal images of live/dead assay at days 1 and 7, beta cells were able to form multicellular aggregates or spheroids. Depicted in more detail in Figure 1(d)-iii, these advantageous beta cells' conformations seem to have been favored by the presence of RGD. In Alg-0 condition, many individualized cells were still observed (Figure 1(d)-i).

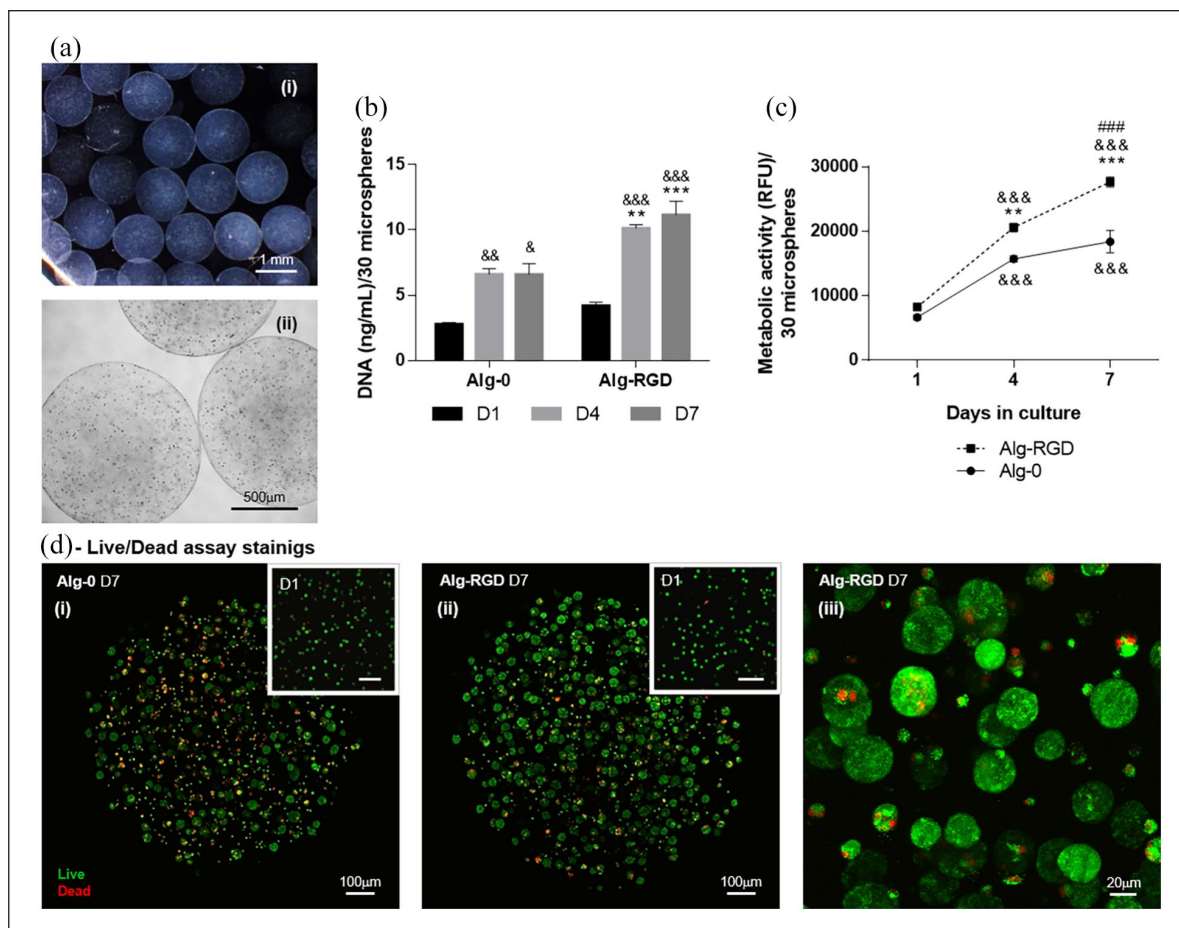


Figure 1. Alginate microspheres characterization and encapsulated INS-1E cells behavior. (a) Microsphere (i) stereoscopic and (ii) inverted optical microscopic imaging illustrating spherical shape, uniform size (average diameter of $1270 \pm 69 \mu\text{m}$), and uniform distribution of INS-1E cells. Effect of RGD on (b) cell proliferation assessed by dsDNA quantification and (c) metabolic activity assessed by resazurin assay at days 1, 4, and 7, and on (d) viability assessed by live/dead assay at days 1 and 7. (i) Alg-0; (ii) Alg-RGD; (iii) Alg-RGD, detail of beta-cells spheroids at higher magnification.

Data are presented as mean \pm SEM ($n = 3$). ** $p < 0.01$, *** $p < 0.001$ Alg-0 vs Alg-RGD; & $p < 0.05$, && $p < 0.01$, &&& $p < 0.001$ D4/D7 vs D1; #### $p < 0.001$ D7 vs D4.

Effect of RGD-grafted alginate on insulin secretion and insulin-related gene expression of encapsulated INS-1E cells

Insulin secretion, the pivotal role of beta cells, was also positively influenced by adhesive peptides. Figure 2(a) shows glucose-mediated insulin secretion from INS-1E cells was improved by presence of RGD peptides, especially when cells were exposed to high glucose concentration stimulus. In presence of the same number of cells, in Alg-RGD condition, insulin secretion increased 2.5-fold between low and high glucose stimuli ($p < 0.001$) whereas it increased only 1.4-fold ($p < 0.05$) in Alg-0. Although there was no glucose stimulation for this assay and only basal insulin was measured, cells with RGD showed a tendency of increased mRNA average expression of genes involved in insulin secretory machinery such as insulin (*Ins1*), pancreatic and

duodenal homeobox (*Pdx1*), glucose transporter 2 (*Glut2*), and sulfonylurea receptor (*Sur1*) (Figure 2(b)), following the insulin secretion profile.

Effect of RGD-grafted alginate on the expression of ECM components of encapsulated INS-1E cells

The incorporation of RGD peptides seems to induce the ability of INS-1E cells to produce endogenous ECM. In fact, a tendency to increased gene expression of matrix components, including collagen type 1 (*Col1a1*), collagen type IV (*Col4a1*), laminin (*Lama1*), and fibronectin (*Fn1*) was observed when RGD was present in the hydrogel as compared to the RGD-free counterpart (Figure 2(c)). mRNA expression of integrin receptors in Alg-RGD showed the same trend, particularly for integrin $\alpha 3$ (Figure 2(c)).

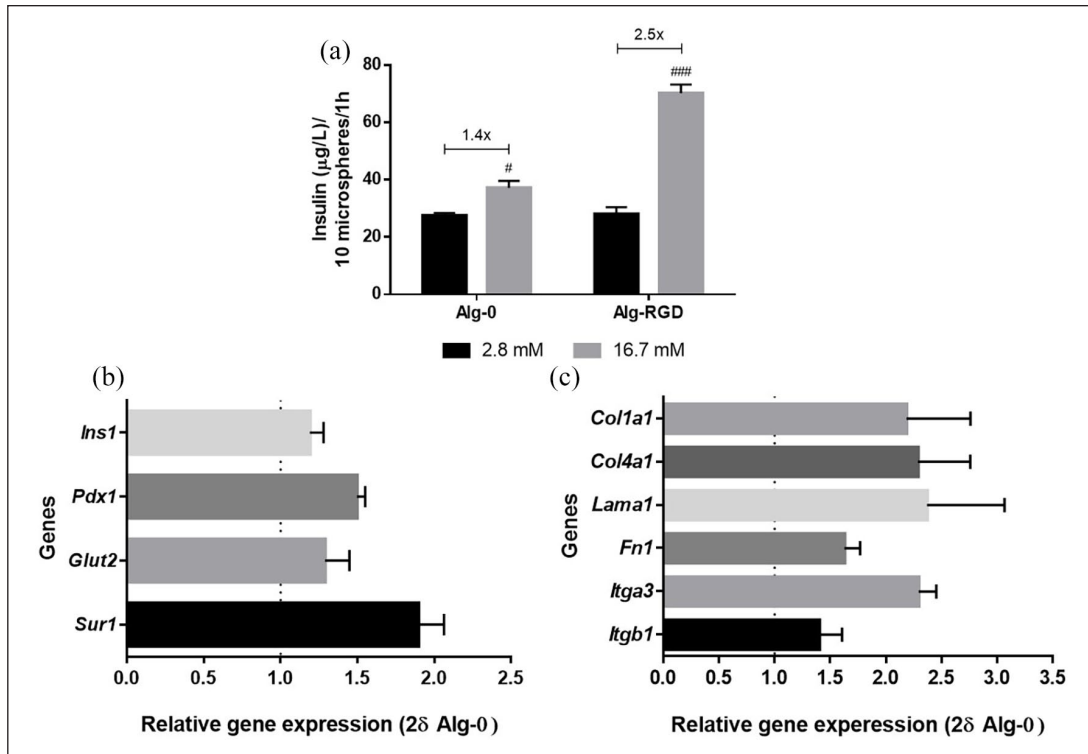


Figure 2. Effect of RGD on encapsulated INS-IE cells insulin secretion, expression of genes of insulin secretion machinery and genes from extracellular matrix components. (a) Levels of insulin, with respective fold increase values, at day 4 of culture, after glucose-stimulated insulin secretion assay (2.8 mM and 16.7 mM glucose stimuli). (b, c) qRT-PCR analysis of gene expression of insulin (*Ins1*), pancreatic and duodenal homeobox 1 (*Pdx1*), glucose transporter 2 (*Glut2*), and sulfonylurea receptor (*Sur1*), relative to the *Hprt1* expression (housekeeping), collagen type I (*Col1a1*), collagen type IV (*Col4a1*), laminin (*Lama1*), fibronectin (*Fn1*), integrin alpha 3 (*Itga3*), and integrin beta 1 (*Itgb1*), relative to *Hprt1* expression (housekeeping) and normalized to expression in condition Alg-0, after 7 days in culture. Data are presented as mean \pm SEM ($n = 3-4$). # $p < 0.05$, ### $p < 0.001$ 2.8 mM vs 16.7 mM.

Glycemic profile, insulin levels, QUICKI and HOMA indexes of diabetic rats implanted with encapsulated INS-IE cells in Alg-RGD model

Aiming to verify surgery-induced variations in rats' diet routine and body weight, animals were weighted and daily food and water intake was evaluated during the whole experimental period (Table 2). Comparing with control rats (GKc), no surgery-induced effects were observed in both body weight and food intake in GKv and GK_i rats. However, water consumption denoted a different profile between groups, confirmed by Kruskal–Wallis test ($p = 0.05$). Notably, GK_i rats showed a trend to decrease water ingestion ($p = 0.09$ between GKc and GK_i), which suggests improved glucose profile. Regarding blood biochemical analyses, no alterations of renal and hepatic parameters were observed, indicating the absence of surgery-induced toxicity (Table 2).

As depicted in Figure 3, glycemic profile of diabetic rats implanted with encapsulated beta cells (GK_i) showed a notable improvement. Occasional glycaemia decreased in both GKv and GK_i rats from 24h after implantation and

was maintained in GK_i during the whole experimental period ($p < 0.01$ in days 3, 4, and 21 and $p < 0.001$ in remaining, compared to GKc rats). On the other hand, the decrease in GKv was transient, possibly related to surgery stress. At the end of experiment GKv glucose values were close to those of GKc and significantly different from those of GK_i ($p < 0.05$) (Figure 3(a)-i). For easy viewing and understanding of this figure, symbols related with statistical significance were not presented. Comparing the occasional (Figure 3(a)-ii) and fasting (Figure 3(b)) glycaemia at the beginning (day 0) and at the end of the experiment (day 21), GK_i rats showed a significant decrease at both levels ($p < 0.05$), being lower than GKc rats' values at the same day ($p < 0.05$). Moreover, occasional and fasting glycaemia depicted respectively average values of 119 mg/dL and 142 mg/dL, which are below of thresholds for diabetes (≥ 126 mg/dL and ≥ 200 mg/dL, respectively). Figure 3(d) shows IPGTT before (day 0) and 7 days after implantation (day 7). Both GKc and GKv groups did not change their glucose levels, whereas GK_i rats showed an improvement of glycaemia 2 h after glucose load ($p < 0.05$). The between-group comparison in glucose at each

Table 2. Body weight, diet routine, and blood biochemical analyses.

Parameter		GKc	GKv	GKi
Body weight (g)	D0	381.67 ± 7.13	373.00 ± 7.94	350.33 ± 2.33
	D21	394.67 ± 1.33	375.67 ± 7.45	356.00 ± 4.93
Food (g/rat/day)		26.38 ± 1.43	25.67 ± 0.71	24.95 ± 1.78
Water (mL/rat/day)		45.67 ± 4.43	43.10 ± 10.95	25.56 ± 1.63
Urea nitrogen (mg/dL)		14.7 ± 0.74	13.7 ± 0.19	16.4 ± 1.19
Creatinine (mg/dL)		0.4 ± 0.04	0.4 ± 0.06	0.4 ± 0.04
Urates (mg/dL)		1.4 ± 0.11	1.2 ± 0.15	1.7 ± 0.23
Total proteins (g/dL)		6.2 ± 0.05	6.0 ± 0.12	5.9 ± 0.11
Albumin (g/dL)		3.1 ± 0.05	3.1 ± 0.06	3.1 ± 0.06
Alanine transaminase (U/L)		45.3 ± 1.15	51.7 ± 3.84	55.5 ± 11.64
Aspartate transaminase (U/L)		127.7 ± 12.42	107.3 ± 11.86	117.0 ± 15.56
Alkaline phosphatase (U/L)		264.5 ± 56.93	236.0 ± 14.73	250.8 ± 30.52
Total bilirubin (mg/dL)		0.2 ± 0.00	0.2 ± 0.00	0.2 ± 0.00

For three experimental groups of diabetic rats, food and water intake were evaluated, per rat per day, during the whole experimental period. At the beginning (D0) and at the end (D21), the body weight was evaluated. Also at day 21 rats were fasted during 6h, and blood samples were collected to evaluate biochemical parameters related to kidney and hepatic function. Data are presented as mean ± SEM ($n = 3-4$). GKc, GK control, GKv, GK vehicle, and GKi, GK implanted.

time-point of IPGTT before (D0) and after (D7) implantation, corrected for interindividual variability glucose tolerance (Figure 3(c)), confirms that only GKi decreased 2 h glucose levels, comparing both with GKc ($p < 0.05$) and GKv ($p < 0.01$). Despite no alterations between groups were observed in fasting insulin levels (Figure 3(e)), improvements of insulin sensitivity index (QUICKI) ($p < 0.05$) and insulin resistance index (HOMA) ($p < 0.05$) were observed in GKi rats, when compared to GKc rats (Figure 3(f) and (g)).

Histologic analyses

After 21 days of subcutaneously implantation, hydrogels and surrounding tissues were removed, fixed and used for histological analyses. Figure 4 shows the implant site and adjacent structures (skin, subcutaneous tissue and muscle) of both control and implanted rats. A thin membrane of collagen surrounding the implanted hydrogels was observed (Figure 4(a)-ii and (b)-ii, black filled arrow). In more detail (Figure 4(c) and (d)), independent of absence or presence of INS-1E beta cells (GKv and GKi, respectively), this membrane shows a moderate inflammatory infiltrate (white asterisks), usually reported in this type of procedures. However, this membrane showed to be well vascularized, with a presence of many microvessels (white arrows). Regarding the implanted beta cells, they notably show a positive staining for insulin, indicating the viability and insulin production activity of these cells (Figure 4(e)). Unlike the *in vitro* findings, INS-1E cells were not able to form pseudo-islets spheroids while implanted in rats, and only a few INS-1E agglomerates were detected inside the hydrogels (Figure 4(d)-2, black dashed arrow).

Discussion

Clinical application of bioartificial pancreas will greatly improve quality of life of diabetic patients worldwide. A crucial aspect to ameliorate function of hydrogel-encapsulated beta cells is the establishment of appropriate niche to support interactions between cells and ECM components, mimicking the complex *in vivo* 3D microenvironment.^{4,5} The proposed model of RGD-grafted alginate hydrogel demonstrated to be an adequate *in vitro* niche for promoting beta cells' viability, proliferation and activity, namely by improving their key role of insulin secretion. The inability of beta cells to produce their own basement membrane elements, reported by others,⁷ seems to be overcome with our model, which was able to promote cell-matrix interactions, not only with incorporated RGD but also with newly expressed endogenous ECM components.

The presence of adhesive peptides also favored assembly of cells into spheroids, leading to better performance observed in beta cells in this condition, namely in terms of insulin secretion. This conformation, also named pseudo-islets, is an essential configuration for proper beta cell functioning and was already demonstrated to improve beta cell performance.³⁵ Chowdhury et al. compared the behavior of MIN6 beta cells dispersed in monolayers or aggregated in pseudo-islets conformation and showed that latter architecture was critical for proper beta cell functioning, ameliorating insulin secretion ability to values superimposable to those observed in human islets.³⁵ This ability of cellular organization, enhanced by the ECM-enriched environment, boosts the usefulness of single beta cells instead of islets, which are restricted to donors' availability.

Previous studies including RGD in 3D models for bioartificial pancreas already demonstrated their beneficial

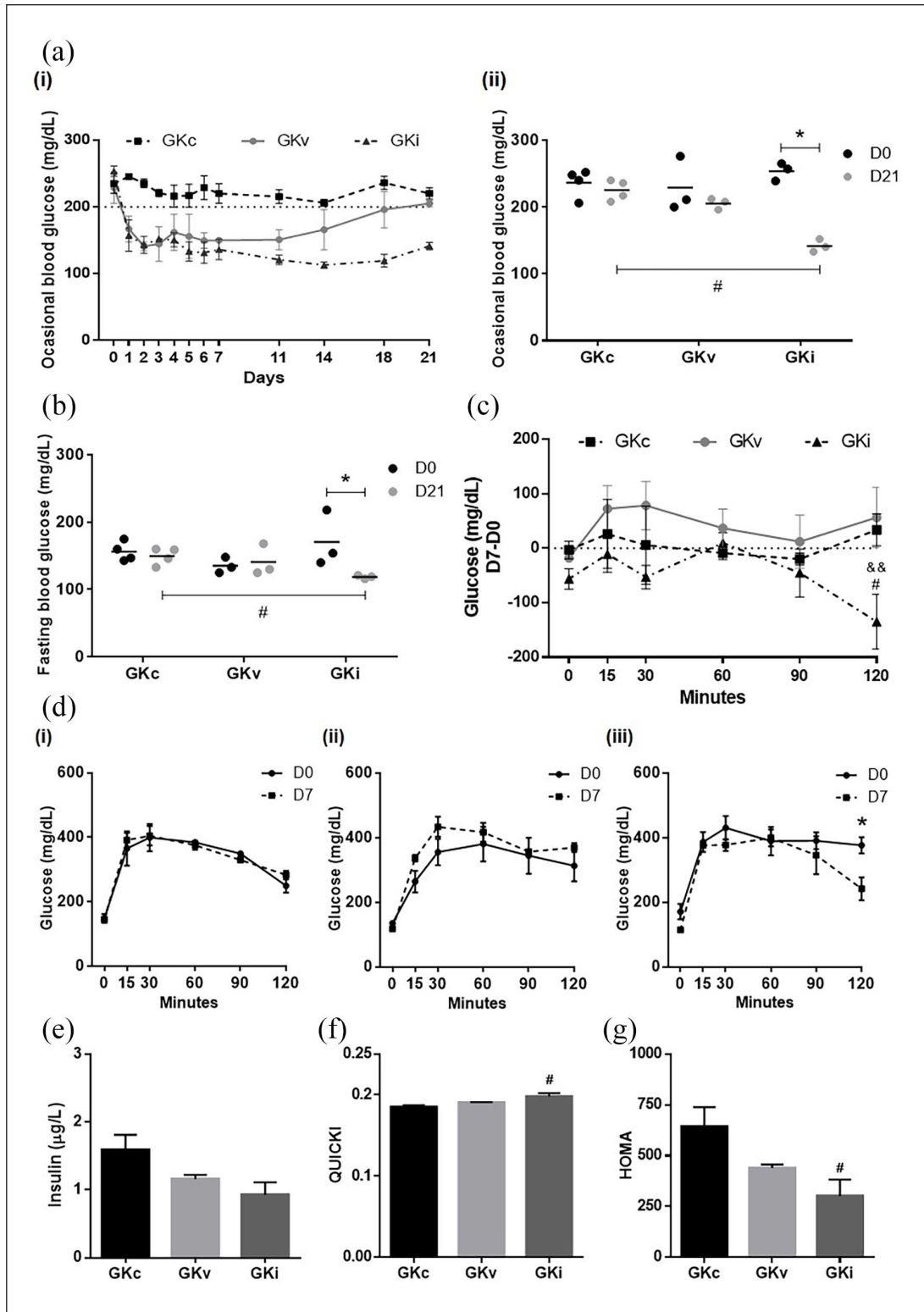


Figure 3. Effect of encapsulated INS-IE cells implantation in glycemic and insulinemic profile of diabetic rats. (a) Occasional blood glucose levels (i) before implantation and during the whole experimental period after implantation and (ii) at day 0 and day 21. (b) Fasting blood glucose levels at day 0 and day 21. (c) Between-group comparison in glucose difference between D7 and D0 in intraperitoneal glucose tolerance test (IPGTT). (d) Group-specific glucose up to 120 minutes after glucose injection, before (D0) and after (D7) implantation, for (i) GK control (GKc), (ii) GK implanted with empty spheres (GKv) and (iii) GK implanted with beta cells (GKI). (e) Insulin levels, (f) QUICKI, and (g) HOMA indexes at the end of the experiment. Data are presented as mean \pm SEM ($n = 3-4$) * $p < 0.05$ D7/D21 vs D0; # $p < 0.05$ GKI vs GKc, && $p < 0.01$ GKI vs GKv.

effects, although using higher peptide's concentration than the one used in this study, which is an indication of high efficiency of our model. In RGD-modified PEGDA hydrogels, the RGD concentration reported to increase insulin secretion was 25-fold higher than the one used in our model.^{13,26} In a recent study, Llacua et al. demonstrated, in alginate hydrogels, an improvement in glucose induced insulin secretion mainly when islets were co-encapsulated with RGD at 1000 μM .²⁷ In our alginate model, the improvement in ECM environment was carried out by introducing RGD at 200 μM , indicating its effectiveness. In the presented approach, RGD peptides were introduced by carbodiimide chemistry, building a more reliable model in which low concentration of peptides are covalently linked to alginate backbone, in contrary to the mentioned study, where ECM components were only physically entrapped in hydrogels.²⁷ Moreover, by using fewer chemical linking sites with RGD we could covalently link other biological entities of interest to further functionalize our alginate model and enhance its properties. Also different from the same study,²⁷ the success of our approach was validated *in vivo*.

In vitro comparison between two experimental conditions (Alg-0 and Alg-RGD) validates the success of RGD effects in cellular outcome, motivating us to allotransplant this RGD-enriched model into type 2 diabetes rats. *In vivo*, our pivotal model for diabetes treatment showed to improve the glycemic profile of diabetic rats. Rats' body weight maintenance during the whole experimental period sets aside the hypothesis of weight loss influence on insulin resistance and suggests the better efficiency of insulin secreted from encapsulated cells. Fasting insulin levels did not change but, in fact, this measurement does not reflect hormone secretion after a meal. Insulin positive immunostaining observed in histological analysis helped to dispel our doubts about the improvement of glycemic profile. Additionally, rats demonstrated to improve their insulin sensitivity. This hormone was used more properly, leading to decreased levels of fasting and occasional glycaemia as well as to a better performance in glucose tolerance test. Our results demonstrated the RGD-enriched hydrogel model efficacy *in vivo* and revealed the positive effect and usefulness of this methodology also in type 2 diabetes. Actually, the application of bioartificial

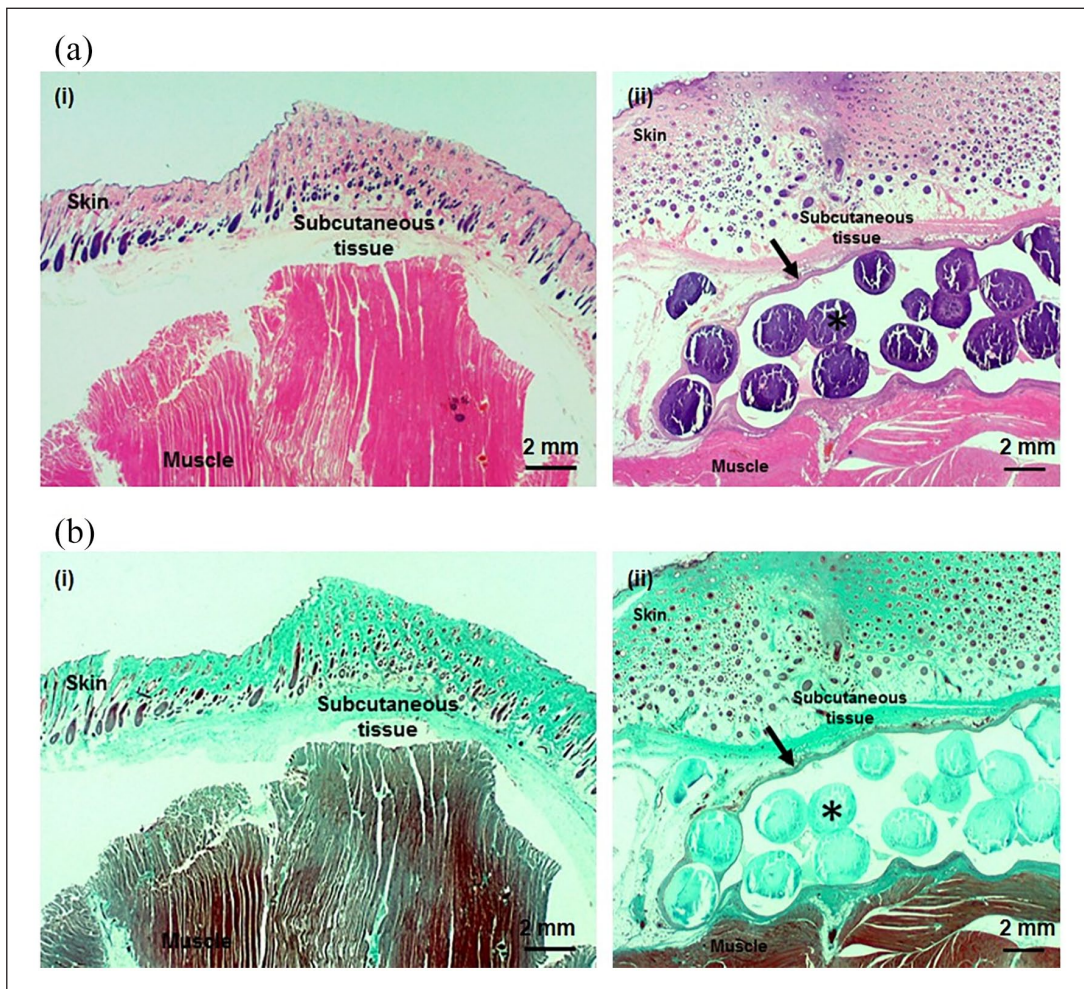


Figure 4. (Continued)

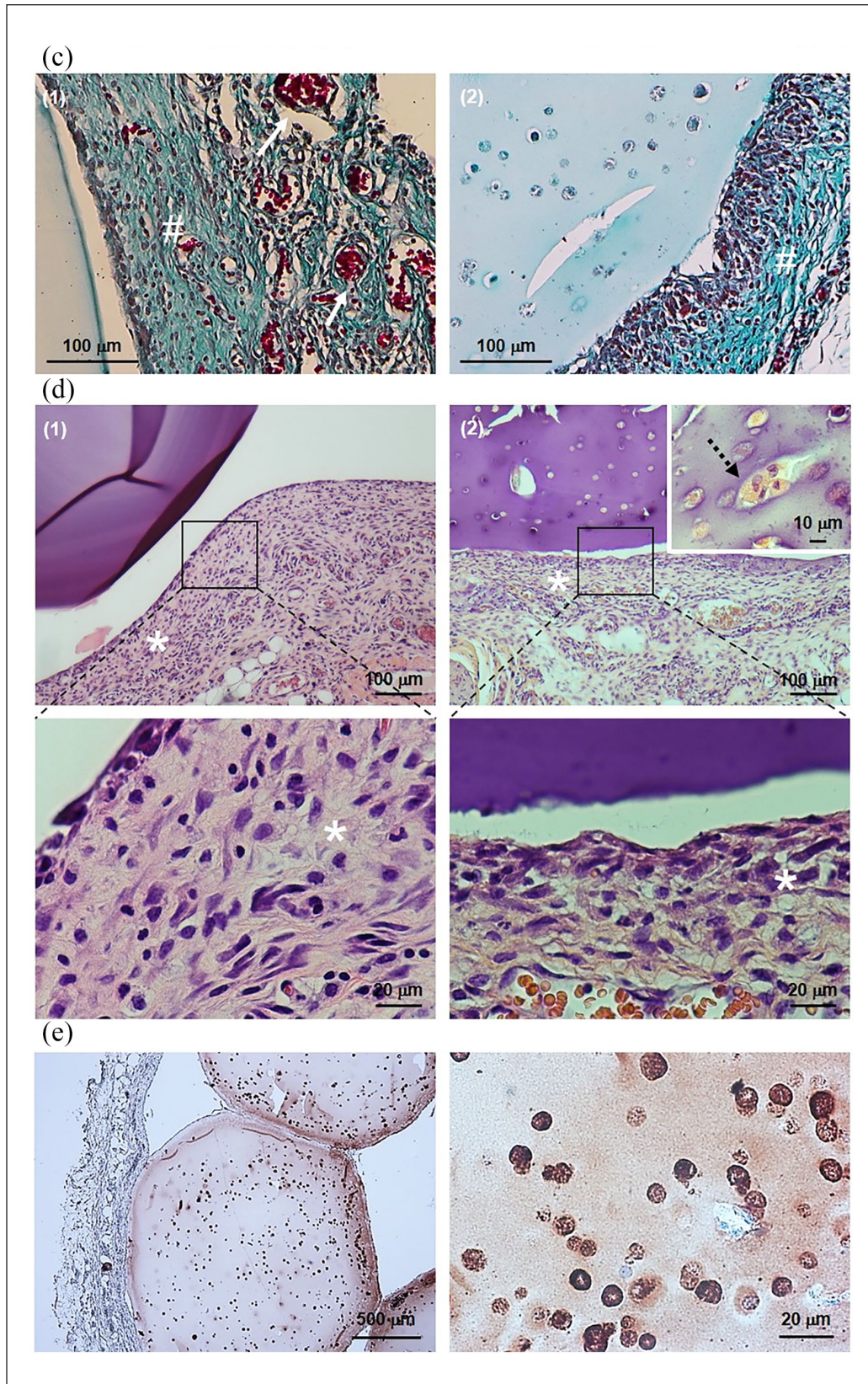


Figure 4. Histological images of implant and surrounding tissues. (a, d) Hematoxylin-eosin staining, (b, c) Masson's trichrome staining, and (e) insulin immunostaining. (i) Control rats; (ii) implanted rats; (1) empty alginate-RGD hydrogels; (2) alginate-RGD hydrogels with beta cells; black asterisks: alginate-RGD hydrogels; black filled arrow: collagen membrane; white arrows: microvessels; black asterisks: collagen deposition; white asterisks: inflammatory infiltrate; black dashed arrow: INS-IE spheroids.

pancreas has only been reported in type 1 diabetes recipients, triggered by its incapacity of insulin production.^{16,36} As to our knowledge, there are no studies elucidating the application of this methodology in type 2 diabetes, even if some authors highlighted the positive outcome of insulin therapy at early stages and its administration becomes mandatory in advanced stages of the disease.

Conclusion

The developed alginate-RGD model demonstrated to be a good *in vitro* niche for supporting beta cells functionality, improving their insulin secretion capacity. *In vivo*, our model showed to improve glycemic profile of diabetic rats, where insulin secreted from encapsulated cells was more efficiently used. For the first time, the beneficial use of bioartificial pancreas in type 2 diabetes was demonstrated.

In future studies, we aim to improve the performance of our model, by reducing hydrogels size and maintaining encapsulated cells in culture until its proliferation and organization into advantageous pseudo-islets configuration.

Concluding, the proposed system stands out as a promising approach to improve beta cells survival and function and increase the success of this therapeutic strategy to treat diabetes.

Author's note

Cristina C Barrias and Raquel Seiça jointly supervised this work.

Acknowledgements

The present work is a collaboration between IBILI (Faculty of Medicine of Coimbra) and INEB (i3S Research Unit from Porto), which are supported by FCT, the Portuguese Foundation for Science and Technology.

Declaration of conflicting interests

The author(s) declared no potential conflicts of interest with respect to the research, authorship, and/or publication of this article.

Funding

The author(s) disclosed receipt of the following financial support for the research, authorship, and/or publication of this article: This work was supported by FCT/MEC through National Funds and co-financed by FEDER through the PT2020 Partnership Agreement under the 4293 Unit I&D, FCT Strategic Project PEst-C/SAU/UI3282/2011-2013 and UID/NEU/04539/2013, FCT in the framework of project UID/BIM/04293/2013, FCT in the framework of project IF/00939/2013/CP1179/CT0001, FCT for Joana Crisóstomo (grant number SFRH/BD/72964/2010), FCT for Sílvia J Bidarra (grant number SFRH/BPD/80571/2011), and FCT and POPH/ESF (EC) for Cristina C Barrias research position FCT Investigator (IF2013).

Note

Part of the results of the present work was presented at the 10th International Conference on Advanced Technologies &

Treatments for Diabetes and published as an abstract in *Diabetes Technology & Therapeutics* (Vol. 19, Suppl. 1, 2017).

References

1. Crisóstomo J, Coelho J and Seiça R. Bioartificial pancreas: in the road to clinical application. In: J Coelho (ed) *Drug delivery systems: advanced technologies potentially applicable in personalised treatment*. Dordrecht: Springer, 2013, pp.127-151.
2. Weir G. Islet encapsulation: advances and obstacles. *Diabetologia* 2013; 56: 1458–1461.
3. Wang R and Rosenberg L. Maintenance of beta-cell function and survival following islet isolation requires re-establishment of the islet-matrix relationship. *J Endocrinol* 1999; 163: 181–190.
4. Cheng JYC, Raghunath M, Whitelock J, et al. Matrix components and scaffolds for sustained islet function. *Tissue Eng Part B Rev* 2011; 17: 235–247.
5. Lin C-C and Anseth KS. Cell-cell communication mimicry with poly(ethylene glycol) hydrogels for enhancing β -cell function. *PNAS* 2011; 108: 6380–6385.
6. Rozario T and Desimone DW. The extracellular matrix in development and morphogenesis: a dynamic view. *Dev Biol* 2010; 341: 126–140.
7. Nikolova G, Jabs N, Konstantinova I, et al. The vascular basement membrane: a niche for insulin gene expression and β cell proliferation. *Dev Cell* 2006; 10: 397–405.
8. Daoud J, Petropavlovskaja M, Rosenberg L, et al. The effect of extracellular matrix components on the preservation of human islet function in vitro. *Biomaterials* 2010; 31: 1676–1682.
9. Kaido T, Yebra M, Cirulli V, et al. Impact of defined matrix interactions on insulin production by cultured human beta-cells: effect on insulin content, secretion, and gene transcription. *Diabetes* 2006; 55: 2723–2729.
10. Pinkse GG, Bouwman WP, Jiawan-Lalai R, et al. Integrin signaling via RGD peptides and anti-beta1 antibodies confers resistance to apoptosis in islets of Langerhans. *Diabetes* 2006; 55: 312–317.
11. Weber LM, Hayda KN and Anseth KS. Cell-matrix interactions improve beta-cell survival and insulin secretion in three-dimensional culture. *Tissue Eng Part A* 2008; 14: 1959–1968.
12. Beenken-Rothkopf LN, Karfeld-Sulzer LS, Davis NE, et al. The incorporation of extracellular matrix proteins in protein polymer hydrogels to improve encapsulated beta-cell function. *Ann Clin Lab Sci* 2013; 43: 111–121.
13. Weber LM and Anseth KS. Hydrogel encapsulation environments functionalized with extracellular matrix interactions increase islet insulin secretion. *Matrix Biol* 2008; 27: 667–673.
14. Sun J and Tan H. Alginate-based biomaterials for regenerative medicine applications. *Materials* 2013; 6: 1285–1309.
15. De Vos P, Faas MM, Strand B, et al. Alginate-based microcapsules for immunoisolation of pancreatic islets. *Biomaterials* 2006; 27: 5603–5617.
16. Qi M. Transplantation of encapsulated pancreatic islets as a treatment for patients with type 1 diabetes mellitus. *Adv Med.* 2014; 2014: 429710.

17. Bidarra S, Barrias C, Fonseca K, et al. Injectable in situ crosslinkable RGD-modified alginate matrix for endothelial cells delivery. *Biomaterials* 2011; 32: 7897–7904.
18. Guerreiro S, Oliveira M, Barbosa M, et al. Neonatal human dermal fibroblasts immobilized in RGD-alginate induce angiogenesis. *Cell Transplant* 2014; 23: 945–957.
19. Maia F, Lourenço A, Granja P, et al. Effect of cell density on mesenchymal stem cells aggregation in RGD-alginate 3D matrices under osteoinductive conditions. *Macromol Biosci* 2014; 14: 759–771.
20. Maia F, Fonseca K, Rodrigues G, et al. Matrix-driven formation of mesenchymal stem cell-extracellular matrix microtissues on soft alginate hydrogels. *Acta Biomater* 2014; 10: 3197–3208.
21. Maia F, Barbosa M, Gomes D, et al. Hydrogel depots for local co-delivery of osteoinductive peptides and mesenchymal stem cells. *J Control Release*. 2014; 189: 158–168.
22. Ruoslahti E. RGD and other recognition sequences for integrins. *Annu Rev Cell Dev Biol* 1996; 12: 697–715.
23. Kuehn C, Dubiel EA, Sabra G, et al. Culturing INS-1 cells on CDPGYIGSR-, RGD- and fibronectin surfaces improves insulin secretion and cell proliferation. *Acta Biomater* 2012; 8: 619–626.
24. Lim DJ, Antipenko SV, Vines JB, et al. Improved MIN6 b-Cell function on self-assembled peptide amphiphile nanomatrix inscribed with extracellular matrix-derived cell adhesive ligands. *Macromol Biosci* 2013; 13: 1404–1412.
25. Lee K-M, Jung G-S, Park J-K, et al. Effects of Arg-Gly-Asp-modified elastin-like polypeptide on pseudoislet formation via up-regulation of cell adhesion molecules and extracellular matrix proteins. *Acta Biomater* 2013; 9: 5600–5608.
26. Weber LM, Hayda KN, Haskins K, et al. The effects of cell-matrix interactions on encapsulated beta-cell function within hydrogels functionalized with matrix-derived adhesive peptides. *Biomaterials* 2007; 28: 3004–3011.
27. Llacua A, de Haan BJ, Smink SA, et al. Extracellular matrix components supporting human islet function in alginate-based immunoprotective microcapsules for treatment of diabetes. *J Biomed Mater Res* 2016; 104: 1788–1796.
28. Dang TT, Xu Q, Bratlie KM, et al. Microfabrication of homogenous, asymmetric cell-laden hydrogel capsules. *Biomaterials* 2009; 30: 6896–6902.
29. Bloch K, Bloch O, Tarasenko I, et al. A strategy for the engineering of insulin producing cells with a broad spectrum of defense properties. *Biomaterials* 2011; 32: 1816–1825.
30. Merglen A, Theander S, Rubi B, et al. Glucose sensitivity and metabolism-secretion coupling studied during two-year continuous culture in INS-1E insulinoma cells. *Endocrinology* 2004; 145: 667–678.
31. Rowley JA, Madlambayan G and Mooney DJ. Alginate hydrogels as synthetic extracellular matrix materials. *Biomaterials* 1999; 20: 45–53.
32. Evangelista M, Hsiong S, Fernandes R, et al. Upregulation of bone cell differentiation through immobilization within a synthetic extracellular matrix. *Biomaterials* 2007; 28: 3644–3655.
33. Fonseca KB, Bidarra SJ, Oliveira MJ, et al. Molecularly designed alginate hydrogels susceptible to local proteolysis as three-dimensional cellular microenvironments. *Acta Biomater* 2011; 7: 1674–1682.
34. Bidarra S, Barrias C, Barbosa M, et al. Immobilization of human mesenchymal stem cells within RGD-grafted alginate microspheres and assessment of their angiogenic potential. *Biomacromolecules* 2010; 11: 1956–1964.
35. Chowdhury A, Dyachok O, Tengholm A, et al. Functional differences between aggregated and dispersed insulin-producing cells. *Diabetologia* 2013; 56: 1557–1568.
36. De Souza YEDM, Chaib E, de Lacerda PG, et al. Islet transplantation in rodents. Do encapsulated islets really work? *Arq Gastroenterol* 2011; 48: 146–152.